Article

J. Biol. Regul. Homeost. Agents. 2024; 38(8): 5711–5720
https://doi.org/10.23812/j.biol.regul.homeost.agents.20243808.458

Effect of Squalene Synthase on Malignant Phenotypes and Anti-Cancer Effect of Celastrol on Prostate Cancer Cells

Lin Yang[1,2,†], Yufang Wang[1,†], Xue Zhang[3], Feng Xu[2], Shuya Ji[2], Jiajia Liu[4], Banglan Cai[1], Bin Peng[1,5,§], Denghai Zhang[1,5,§], Yong Li[2,*]

[1]Postgraduate Training Base in Shanghai Gongli Hospital, Ningxia Medical University, Pudong New Area, 200135 Shanghai, China
[2]Department of Oncology, Shanghai Pudong New Area Gongli Hospital, Secondary Military Medical University, 200135 Shanghai, China
[3]Postgraduate Training Base in Shanghai Gongli Hospital, Ningxia Medical University, College of Basic Medicine, Pudong New Area, 200135 Shanghai, China
[4]School of Medicine, Shanghai University, Baoshan Area, 200444 Shanghai, China
[5]Shanghai Health Commission Key Lab of Artificial Intelligence (AI)-Based Management of Inflammation and Chronic Diseases, Sino-French Cooperative Central Lab, Shanghai Pudong Gongli Hospital, Secondary Military Medical University, Pudong New Area, 200135 Shanghai, China
*Correspondence: liyong_yyll@163.com (Yong Li)
[†]These authors contributed equally.
[§]These authors contributed equally.
Submitted: 12 June 2023 Revised: 11 October 2023 Accepted: 17 October 2023 Published: 1 August 2024

Background: Prostate cancer (PC) is one of the most common malignant tumors, and the effect of celastrol on squalene synthase (SQS) in PC is unknown. This study aimed to investigate the effect of celastrol on SQS in PC.
Methods: The protein expression was detected by Western blot. Cell proliferation capacity was detected by cell counting kit-8 (CCK-8) kit (450 nm optical density values). Cell scratch (wounding healing rate) and transwell assays (migration cells number) detected the cells' migration abilities. Messenger RNA (mRNA) expression was detected using a real-time polymerase chain reaction test.
Results: Celastrol decreased the expression of SQS in PC cells, and the knockdown of the SQS-encoding gene farnesyl-diphosphate farnesyltransferase 1 (*fdft1*) with and without celastrol treatment decreased PC cell proliferation and migration abilities. Furthermore, overexpression of the *fdft1* gene attenuated the proliferation and migration abilities of PC-3 cells. Treatment with celastrol with *fdft1* gene overexpression can still decrease the proliferation and migration abilities of PC-3 cells.
Conclusion: This study verified that celastrol decreases the proliferation and migration abilities of PC-3 and Lymph Node Carcinoma of the prostate (LNCaP) cells and revealed that celastrol reduces SQS expression. The results indicate that the inhibitory effect of celastrol on the malignant phenotypes of PC cells is partly dependent on SQS, and SQS is involved in the malignant behaviour of PC cells. Furthermore, there may be a dual effect dependent on the SQS protein expression level on the malignant phenotypes of PC cells.

Keywords: prostate cancer; celastrol; squalene synthase; proliferation; migration

Introduction

Prostate cancer (PC) has the second-highest morbidity rate and fifth-highest mortality rate among cancers in humans [1–3]. Therefore, the discovery of a new medicines to treat it have clinical value.

Studies have determined that high cholesterol levels promote PC development [4–7]. Cholesterol-targeted therapy may inhibit the growth of aggressive PC through intracellular steroidogenesis [8–10]. The raw material of cholesterol synthesis, acetyl-Acetoacetyl coenzyme A (CoA), passes through the mevalonate pathway to generate farnesyl pyrophosphate (FPP), which can be metabolised through a sterol or non-sterol pathway. Squalene synthase (SQS) plays a key role in this branch, as it can catalyse the condensation of two molecules of FPP to form squalene [11,12], which is further metabolised to generate cholesterol and is a crucial enzyme in cholesterol synthesis. Studies have demonstrated that downregulating the SQS-encoding gene farnesyl-diphosphate farnesyltransferase 1 (*fdft1*) or inhibiting the expression of SQS can significantly inhibit the proliferation of PC [13]. In PC cells, the activity of SQS and its mediated cholesterol synthesis are the determinants of cholesterol associated with cell membrane microdomains. Therefore, inhibition of SQS may suppress proliferation and induce PC cell death [14,15].

Celastrol, a triterpenoid extracted from the Chinese herbal medicine *Tripterygium wilfordii*, is used in inflam-

Copyright: © 2024 The Author(s). Published by Biolife Sas. This is an open access article under the CC BY 4.0 license.
Note: *J. Biol. Regul. Homeost. Agents.* stays neutral with regard to jurisdictional claims in published maps and institutional affiliations.

Journal of
BIOLOGICAL REGULATORS
and Homeostatic Agents

matory diseases and has therapeutic effects on cancer, neurodegenerative diseases, obesity and atherosclerosis [16, 17]. Studies have demonstrated that celastrol modulates multiple signalling pathways and has anti-tumour efficacy [17]. It also inhibits PC [18–21], although the mechanism remains unclear.

Recent studies have reported that celastrol can inhibit SQS in *Aspergillus flavus*, a type of fungi [22]. However, the regulatory effect of celastrol on human SQS has not been reported. Despite the differences in the amino acid hinge region between humans and fungi, the overall structure of SQS is the same in eukaryotes [23]. This study investigated the effect of SQS on PC cells and the effect of celastrol on SQS.

Materials and Methods

Materials

For this study, prostate cancer cell lines were obtained from the Shanghai Cell Bank (TCHu158: PC-3, TCHu173: Lymph Node Carcinoma of the prostate (LNCaP), Shanghai, China). The cell counting kit-8 (CCK-8) reagent was purchased from Shanghai Qihai Futai Biotechnology (C008-2, Shanghai, China). The small interfering RNA (siRNA)-mate transfection reagent, siRNA transfection sequence and real-time polymerase chain reaction (PCR)-related primers were purchased from Gemma Gene (Shanghai, China), and the siRNA sequences are as follows: 5′-ACTTGCTACAAGTATCTCAAT-3′. The antibody details of the SQS are as follows: SQS (antibody dilution: 1:1000, ab236666, Abcam, Cambridge, UK) and glyceraldehyde-3-phosphate dehydrogenase (GAPDH) antibodies (antibody dilution: 1:1000, GB12002, Servicebio, Wuhan, China). Details of the secondary antibodies are as follows: anti-rabbit immunoglobulin G (IgG) antibody (antibody dilution: 1:5000, A0208, Biyuntian, Shanghai, China) and anti-mouse IgG antibody (antibody dilution: 1:5000, A0216, Biyuntian, Shanghai, China). Plasmid pcDNA3.1-H_FDFT1-EF1-ZsGreen1 and empty vector pcDNA3.1-MCS-EF1-ZsGreen1 were purchased from Jiman Biotechnology (Shanghai, China). Lipofectamine™ 2000 was purchased from Invitrogen (11668030, Waltham, MA, USA), and celastrol (≥98%, high-pressure liquid chromatography, solid) was purchased from SIGMA (C0869, St. Louis, MO, USA).

Cell Culture

RPMI 1640 (12633012, Gibco, Carlsbad, CA, USA) was used, and the medium was supplemented with 10% foetal bovine serum (FBS) (10099, Gibco, Carlsbad, CA, USA). The cell culture media were supplemented with 100 IU/mL of penicillin and 100 µg/mL of streptomycin (product number: 15070063, Gibco, Carlsbad, CA, USA). Cells were cultured at 37 °C in a 5% CO_2 incubator and used for the experiments during the exponential phase [24]. All cells were identified using short tandem repeat (STR) analysis and tested for mycoplasma. The company provided the STR identification report, and mycoplasma testing was performed using a kit (11-9025, Minerva-Biolabs, Berlin, Germany). The results showed no other cell contamination and no mycoplasma contamination of the cells used in this study.

Cell Counting Kit Assay

In total, 5000 cells/well were placed in a 96-well plate, with three duplicate wells in each group, and allowed to adhere. Celastrol (C0869, SIGMA, St. Louis, MO, USA) was then added for 24 and 48 h, respectively. A total of 10 µL of CCK-8 reagent (C008-2, Qihai Futai Biotechnology, Shanghai, China) was added, and the 450 nm optical density (OD) values were measured [24].

Western Blot

Total protein was from the cells after lysing the cells with lysate. The concentration of protein was subsequently detected using bicinchoninic acid (B9643, SIGMA, St. Louis, MO, USA) experiments. Subsequent Western blot experiments were performed using sodium dodecyl-sulfate polyacrylamide gels. Equal amounts of the samples were used during the experiment. Membrane transfer experiments were performed using polyvinylidene fluoride membranes. Blocking was performed after the transfer experiment was completed. The membranes were incubated overnight at 4 °C with primary antibodies. The following day, the corresponding secondary antibody incubation was performed after washing. The cells were then coloured with enhanced chemiluminescence, and images were obtained with a chemiluminescence imager. Finally, ImageJ software (version 1.8.0, LOCI, University of Wisconsin, Madison, WI, USA) was used for semi-quantitative analysis [24].

Small Interfering RNA Transfection

2×10^5 cells/well (PC-3) and 3×10^5 cells/well (LNCaP) were plated into 12-well plates. After 24 h (PC-3) and 48 h (LNCaP), the cell confluency reached approximately 50%. The siRNA-Mate transfection reagent and *fdft1* gene RNA oligo (5′-ACTTGCTACAAGTATCTCAAT-3′) transfection sequences were used to formulate complexes for transfection. The siRNA transfection experiments were divided into two groups: an experimental group (siRNA *fdft1* [siR-*fdft1*]) and a control group (negative control [NC]) [24].

Overexpression of the fdft1 Gene

3×10^5 cells (PC-3) and 4×10^5 cells (LNCaP) were seeded into 12-well plates. After 24 (PC-3 cells) and 48 h (LNCaP cells), the cells were transfected using the FBS-free 1640 basal medium, Lipofectamine™ 2000 transfection reagent (11668030, Thermo Fisher Scientific, Waltham, MA, USA) and recombinant plasmids.

The cells were grouped into three groups: an experimental group (transfection plasmid pcDNA3.1-H_FDFT1-EF1-ZsGreen1), an empty vector group (transfection empty plasmid pcDNA3.1-MCS-EF1-ZsGreen1) and NC group (no plasmid transfection). The transfection complexes were prepared according to the instructions, and 100 µL of the complex was added to each of the wells, which were then placed back into the incubator for culturing. After 48 h transfection, some cells were used to verify the transfection efficiency, and some were used for subsequent experiments [24].

Real-Time Polymerase Chain Reaction

The total RNA of cells was extracted using the RNA extraction kits (B511321, Sango Biotech, Shanghai, China) and then reversed transcribed into complementary DNA. Using the synthesised primers for the target gene, sample preparation and spotting were performed, and three duplicate wells were set up. The reactions were conducted under the following conditions: pre-denaturation at 95 °C for 60 s, denaturation at 95 °C for 15 s, annealing at 60 °C for 15 s and extension at 72 °C for 45 s, for a total of 35 cycles. Using *GAPDH* as a reference, the cycle threshold value of each sample was statistically analysed, and used the $2^{-\Delta\Delta Ct}$ method. The *fdft1* primers were: F: ACCCTGATGATGGATGCCAC and R: AACGACAGGTAGATGGGGGA; the *GAPDH* primers were: F: CATGAGAAGTATGACAACAGCCT and R: AGTCCTTCCACGATACCAAAGT.

Transwell Migration Assay

Cells were trypsinised, centrifuged, and washed twice with phosphate buffer solution (PBS) (806552, SIGMA, St. Louis, MO, USA). Subsequently, 5×10^5 (PC-3) and 10×10^5 cells/mL (LNCaP) were placed in a 24-well culture plate, and 200 µL of cell suspension (approximately 1×10^5 cells for PC-3 cells and 2×10^5 cells for LNCaP cells) was added to the upper chamber. After the PC-3 cells had migrated for 48 h and the LNCaP cells for 72 h, the medium in the upper chamber was aspirated, and the chamber was immersed twice in PBS for gentle washing before being fixed with 4% paraformaldehyde (158127, SIGMA, St. Louis, MO, USA). Following the staining of the cells with 1% crystal violet (46364, SIGMA, St. Louis, MO, USA), cells in the upper chamber were removed, and those present in the subbasement membrane were subsequently observed through a microscope. Three different visual fields were randomly selected under a 100-fold light microscope (Biological positive microscope-53, OLYMPUS, Tokyo, Japan), and the average value was calculated after counting [24].

Scratch Test

PC-3 and LNCaP cells were seeded in 12-well plates for the scratch test. Cell scratches were performed as cells grew and covered the plate's bottom. Images were captured under a 100× optical microscope (Biological positive microscope-53, OLYMPUS, Tokyo, Japan), and the width of the scratch was recorded at 0 h. The cell culture was continued, and images were captured at 24 and 48 h [24].

Statistical Analysis

Data are presented as mean ± standard deviation. *t* test was used for the comparisons of means between two groups, and a one-way analysis of variance (ANOVA) statistical software was used to compare means between three or more groups using SPSS 21.0 (IBM Corp., Chicago, IL, USA); $p < 0.05$ was statistically significant.

Results

The effect of celastrol on SQS expression and the malignant behaviour of PC cells was investigated.

Effect of Celastrol on the Proliferation and Migration of Prostate Cancer Cells

To observe the effect of celastrol on the proliferation of PC cells, PC-3 and LNCaP cells were co-cultured with celastrol for 24 at different concentrations. The results revealed that the cell viability of PC cells decreased gradually with the increase in celastrol concentration. The half-maximal inhibitory concentration of PC-3 cells was 1.93 µM and that of LNCaP cells was 2.00 µM. The cell viability of the two types of cancer cells was significantly decreased (Fig. 1A,B).

Transwell was used to observe cell migration with celastrol treatment. The number of cells passing through the filtration membrane in the drug-treated groups was significantly reduced. The above results demonstrate that 2.00 µM celastrol inhibits the migration of PC cells (Fig. 1C,D).

A scratch test was used to observe cell migration with celastrol treatment. The scratch healing of PC cells decreased significantly, further indicating that celastrol inhibits the migration of these cells (Fig. 1E,F).

Effect of Celastrol on the Expression of Squalene Synthase in Prostate Cancer Cells

The expression of SQS in the two types of cells was detected using Western blot. Compared with the expression of SQS in PC-3 cells, the expression abundance of SQS in LNCaP cells was higher ($^*p < 0.05$). After treatment with celastrol, the expression level of SQS was decreased, and the expression of SQS gradually decreased with increasing celastrol concentrations, indicating that celastrol reduces the expression of SQS in PC cells. The histograms in Fig. 2A–C display the quantitative plots of SQS protein expression.

Journal of
BIOLOGICAL REGULATORS
and Homeostatic Agents

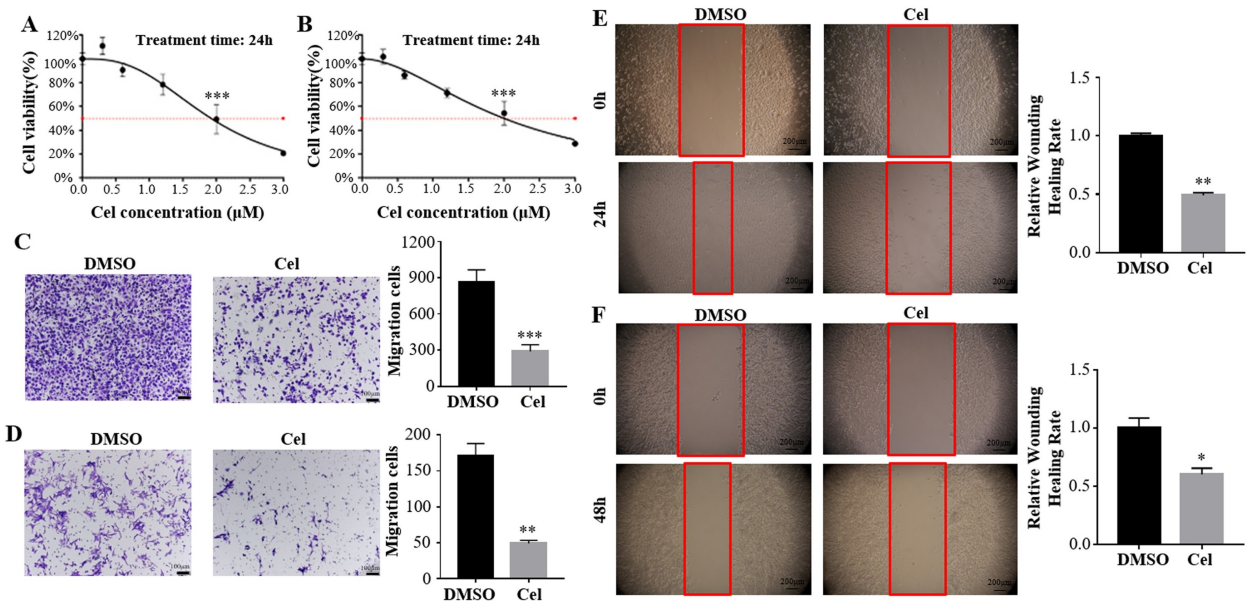

Fig. 1. Effects of celastrol on the proliferation and migration of prostate cancer cells. (A,C,E) PC-3 cells; (B,D,F) LNCaP cells. (A,B) Cell proliferation after co-culture with celastrol at different concentrations. (C,D) Transwell experiment: original magnification ×100. (E,F) Scratch experiment: original magnification ×100. Cell migration after co-culture with celastrol. DMSO: control group. Cel: Drug-treated group. Error bars: mean ± SD, using two-tailed Student's *t* test analysis, $*p < 0.05$, $**p < 0.01$, $***p < 0.001$. PC, prostate cancer; DMSO, dimethyl sulfoxide; SD, standard deviation; LNCaP, Lymph Node Carcinoma of the prostate.

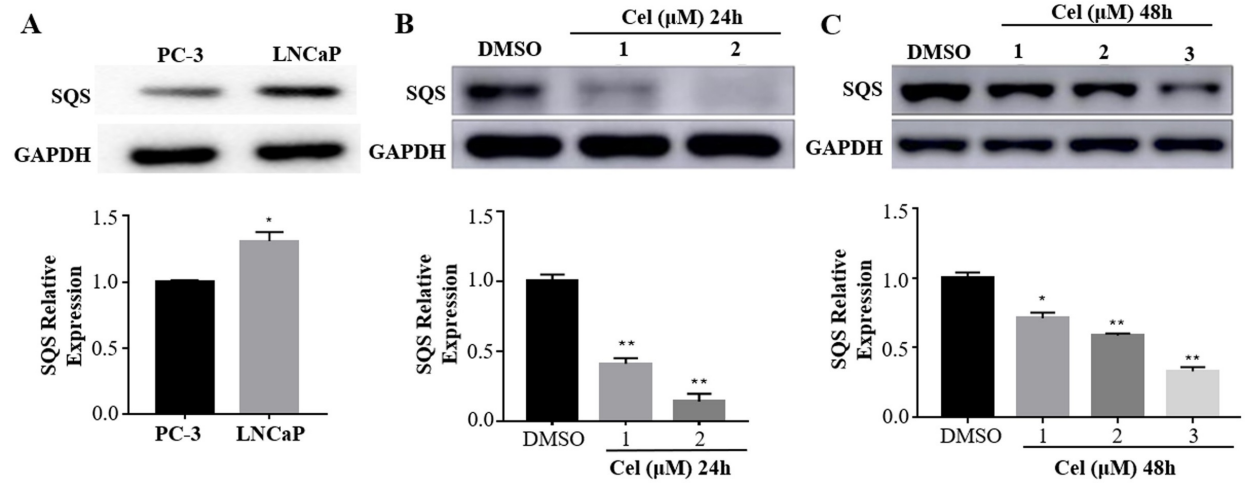

Fig. 2. Effect of celastrol on the expression of squalene synthase in prostate cancer (PC) cells. (A) Expression of SQS in two untreated PC cells was observed using Western blot. Error bars: mean ± SD using two-tailed Student's *t* test analysis. (B) PC-3 cells were treated with 1 and 2 μM of celastrol for 24 h. Error bars: mean ± SD using one-way ANOVA. (C) LNCaP cells were treated with 1, 2 and 3 μM of celastrol for 48 h. DMSO: control group. Cel: Drug-treated group. Error bars: mean ± SD using one-way ANOVA analysis. $*p < 0.05$, $**p < 0.01$. SQS, squalene synthase; ANOVA, analysis of variance; GAPDH, glyceraldehyde-3-phosphate dehydrogenase.

Effect of siRNA fdft1 on the Proliferation and Migration of Prostate Cancer Cells

The expression of the *fdft1* gene in the two cancer cells was manipulated using siRNA, and the changes in the malignant phenotype of cells were observed. The results demonstrated that SQS expression decreased ($**p < 0.01$) (Fig. 3A). Compared with the NC groups, siRNA *fdft1* transfected groups exhibited lower proliferation ability. Af-

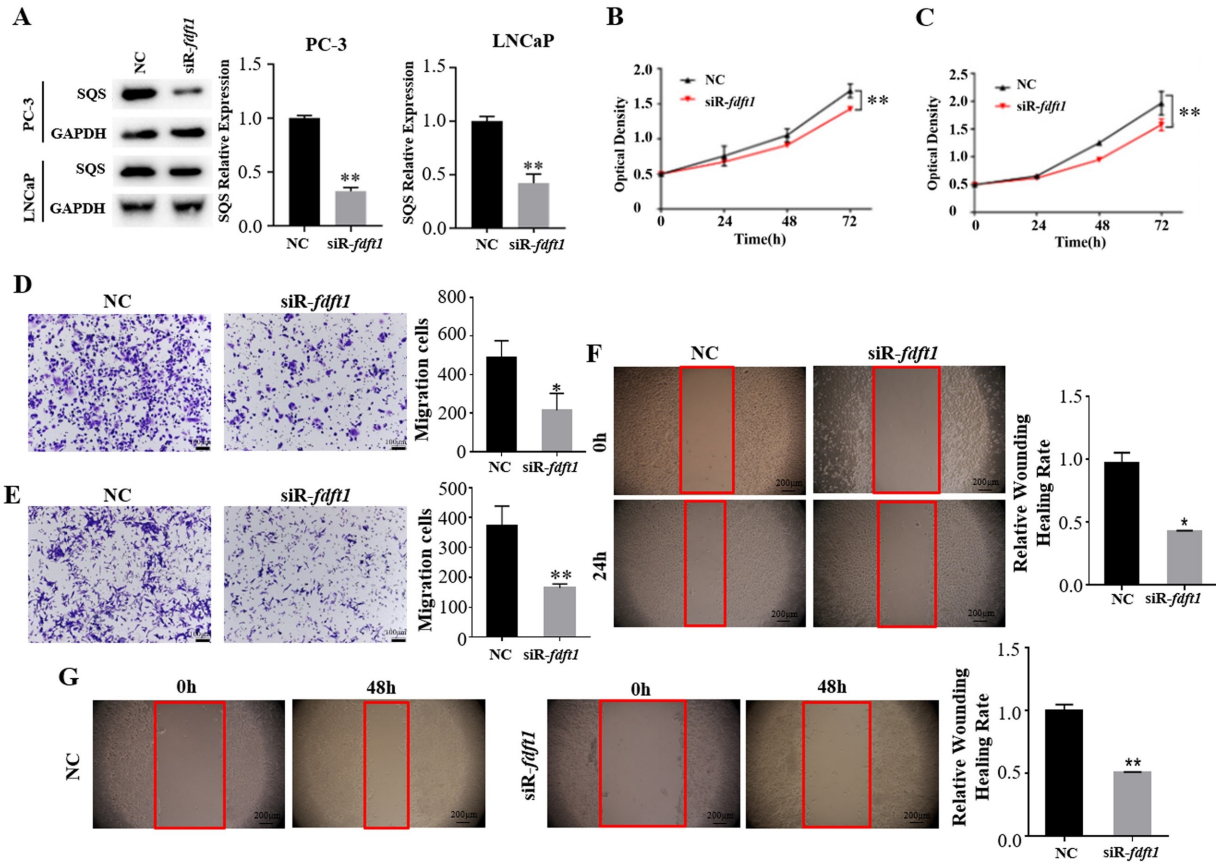

Fig. 3. Effect of siRNA *fdft1* on the proliferation and migration of PC cells. (A) Western blot results of SQS expression. Error bars: mean ± SD using two-tailed Student's *t* test analysis. (B) After transfection, the proliferation of transfected cells was observed using a cell counting kit-8 (CCK-8) assay. (C) CCK-8 assay was used to observe the proliferation changes of the transfected cells. Transwell experiment: original magnification ×100. (D) Successfully transfected PC-3 cells were collected and placed in a transwell chamber for a 48-h migration. (E) Successfully transfected LNCaP cells were collected and placed in a transwell chamber for a 72-h migration. Scratch test: original magnification ×100. (F) After transfection, PC-3 cells underwent a scratch test, and the scratch was left to heal for 24 h. (G) After transfection, LNCaP cells underwent a scratch test, and the scratch was left to heal for 48 h. Error bars: mean ± SD using a two-tailed Student's *t* test analysis, $*p < 0.05$, $**p < 0.01$. siRNA, small interfering RNA; NC, negative control; *fdft1*, farnesyl-diphosphate farnesyltransferase 1.

ter 72 h of proliferation, the OD values of the transfected PC cells were significantly lower, indicating that the reduction in SQS proteins resulting from the introduction of siRNA *fdft1* inhibits the proliferation of the two cancer cells (Fig. 3B,C).

The transwell migration assay results indicated that the numbers of transmembrane cells in the siRNA *fdft1* groups were significantly lower than in the control groups (Fig. 3D,E). The scratch test results revealed that the scratch widths of PC cells after celastrol treatment were significantly larger (Fig. 3F,G). These results demonstrate that siRNA *fdft1* can decrease the migration of the two cancer cells.

Effect of siRNA fdft1 + Celastrol Treatment on the Proliferation and Migration of PC Cells

The PC cells were transfected with siRNA *fdft1* and 2 μM of celastrol for 24 and 48 h, respectively, to observe the changes in SQS protein levels and cell proliferation and migration. No obvious change was identified in the expression of SQS in the transfection group treated with celastrol compared with the control group treated with siRNA alone (Fig. 4A,B). With the increase in proliferation time, the proliferation of both cancer cells in the drug treatment group exhibited a decreasing trend. After 72 h of proliferation, the OD value of the transfection group treated with celastrol was significantly lower than that of the control group (Fig. 4C,D). Transwells were used to examine the migration ability of cells, and the results revealed that the number of cells able to cross the membrane was significantly reduced

Journal of
BIOLOGICAL REGULATORS
and Homeostatic Agents

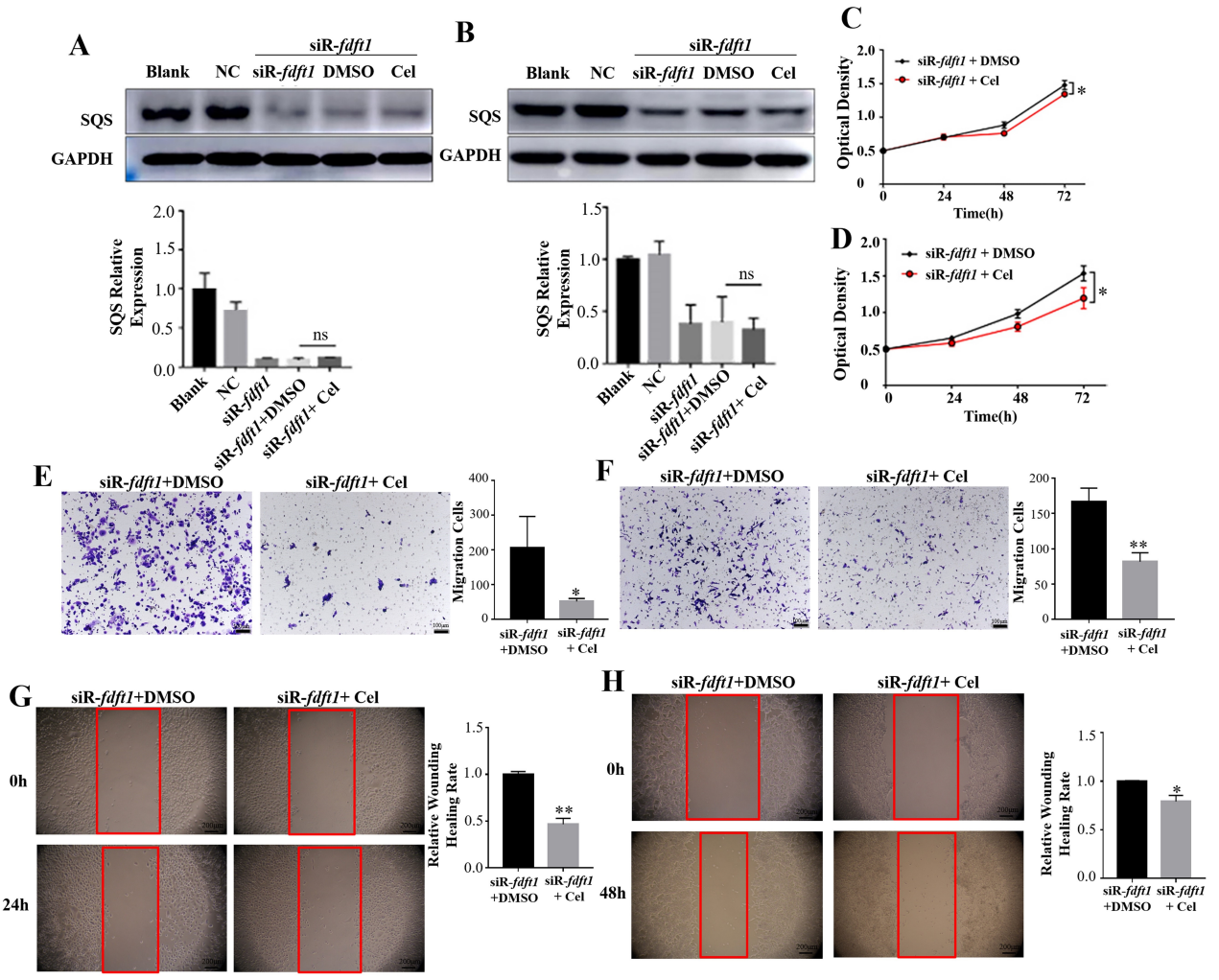

Fig. 4. Effects of siRNA *fdft1* + celastrol on the proliferation and migration of PC cells. (A) Expression of SQS in PC-3 cells following treatment with siR-*fdft1*and 2 μM of celastrol. (B) Expression of SQS in LNCaP cells following treatment with *fdft1*and 2 μM of celastrol. (C) Transfected PC-3 cells were treated with 2 μM of celastrol for 24 h, and CCK-8 assay was used to detect cell proliferation. (D) Successfully transfected LNCaP cells were treated with 2 μM of celastrol, and cell proliferation was observed through a CCK-8. Transwell experiment: Original magnification ×100. (E) Successfully transfected PC-3 cells were treated with 2 μM of celastrol, and cell migration was observed using a transwell assay. (F) Successfully transfected LNCaP cells were treated with 2 μM of celastrol, and cell migration was observed through a transwell assay. Scratch test: Original magnification ×100. (G) Successfully transfected PC-3 cells were treated with 2 μM of celastrol, and cell migration was observed using a scratch test. (H) Successfully transfected LNCaP cells were treated with 2 μM of celastrol, and cell migration was observed through a scratch test. DMSO: control group. Cel: Drug-treated group. Error bars: mean ± SD using a two-tailed Student's *t* test analysis, $*p < 0.05$, $**p < 0.01$, ns, no significant.

after celastrol treatment (Fig. 4E,F). Similarly, the scratch assay results indicated that the scratch width of cells was significantly increased after celastrol treatment (Fig. 4G,H). These results demonstrate that celastrol treatment reduces PC cell migration and invasion ability.

Effect of fdft1 Overexpression on the Proliferation and Migration of PC Cells

The over-expression of the *fdft1* gene in the two cancer cells was demonstrated by Western blot ($**p \leq 0.01$) (Fig. 5A). The OD value of the transfected PC-3 cells was lower. However, in the LNCaP cells, no significant change in the OD value of the transfected group was identified compared with the empty vector group (Fig. 5B,C). The transwell results demonstrated that the number of transmembrane cells in the transfected PC-3 cell experimental group was significantly lower; however, no difference between the experimental group and empty vector group for LNCaP cells was detected in terms of the number of transmembrane cells (see Fig. 5D,E). These results reveal that *fdft1* over-

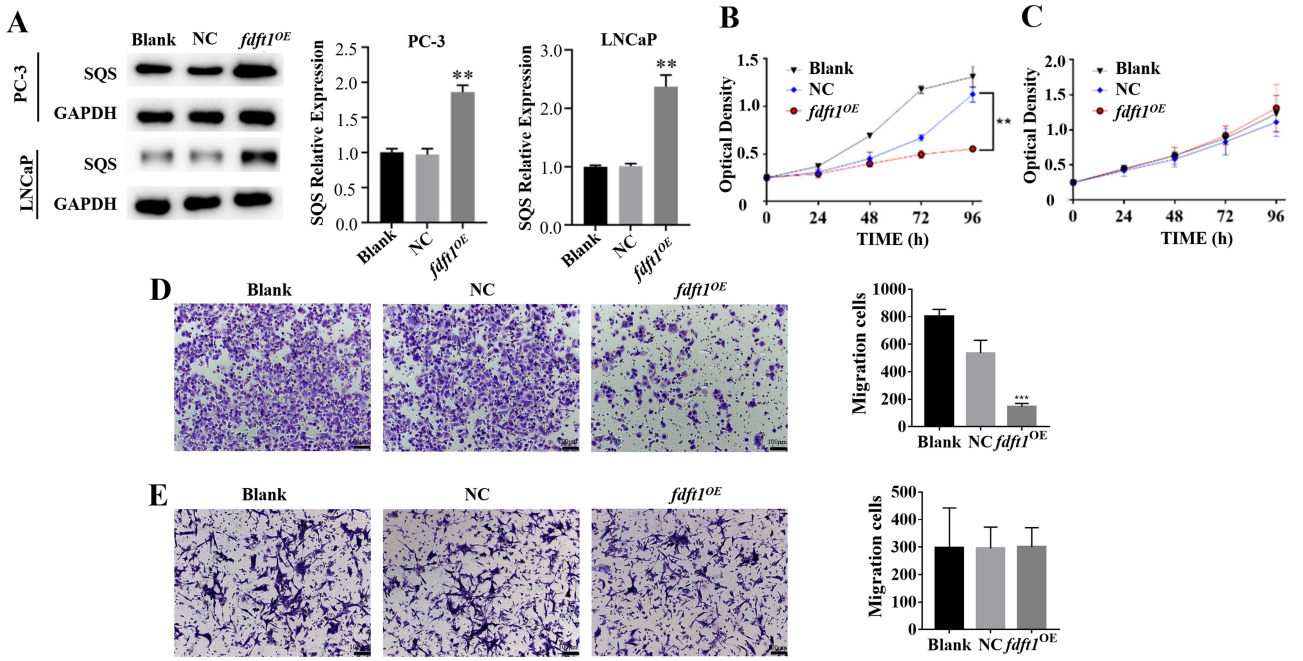

Fig. 5. Effects of overexpression of *fdft1* on the proliferation and migration of PC cells. (A) Western blot results of SQS expression in the empty vector, NC and fdft1 overexpression groups. Error bars: mean ± SD using two-tailed Student's *t* test analysis. (B) PC-3 cells were seeded with 5000 cells/well in a 96-well plate for the CCK-8 assay to observe the proliferation changes after overexpression of *fdft1*. (C) LNCaP cells were seeded with 5000 cells/well in a 96-well plate for the CCK-8 to observe the proliferation changes after overexpression of *fdft1*. Transwell experiment: original magnification ×100. (D) PC-3 cells were transplanted into a transwell chamber with 1×10^5 cells/cell for 48 h. (E) LNCaP cells were transplanted into a transwell chamber with 2×10^5 cells/cell for 72 h. DMSO: control group. Cel: Drug-treated group. Error bars: mean ± SD using two-tailed Student's *t* test analysis, $^{**}p < 0.01$, $^{***}p < 0.001$.

expression inhibits the proliferation and migration of PC-3 cells but has no noticeable effect on LNCaP cells.

Effect of fdft1 Overexpression + Celastrol Treatment on the Proliferation and Migration of PC Cells

The *fdft1* gene was overexpressed in PC-3 cells, which were then treated with 2 μM of celastrol for 24 h, and the changes in protein levels, cell proliferation and migration were observed. No significant change in the expression of SQS in the overexpressed PC-3 cells treated with celastrol was noted compared with the overexpressed control group (Fig. 6A). With the increase in proliferation time, the proliferation of PC-3 cells in the experimental group exhibited a decreasing trend. After 96 h of proliferation, the OD value of the overexpressed group treated with celastrol was significantly lower than that of the control group (Fig. 6B). The inhibition rate of proliferation decreased compared with the non-transfected cells in the previous experiment. The transwell migration assay results revealed that the number of transmembrane cells in the PC-3 experimental group was significantly lower than in the control group (see Fig. 6C). These results indicate that the addition of celastrol and the overexpression of *fdft1* can inhibit the migration of PC-3 cells.

Discussion

In this study, the role of SQS in the malignant phenotype of PC cells was investigated to identify whether the tumour-suppressive effect of celastrol on PC cells is related to its influence on SQS. The results revealed that celastrol reduces the expression of SQS in PC cells and verified that the knockdown of SQS can inhibit the proliferation of these cells. They also demonstrated for the first time that manipulating *fdft1* expression inhibits the migration of PC cells, whereas *fdft1* overexpression inhibits the proliferation and migration of PC-3 cells. In addition to reducing SQS, celastrol can inhibit the proliferation and migration of the two cancer cells after reducing SQS levels, but the inhibition rates are reduced.

The present study demonstrated again the inhibition of celastrol on the malignant behaviour of PC cells, and its results are consistent with those of previous reports [18–22,25–28]. Several studies have reported that celastrol inhibits PC development by regulating micro RNAs [21,25,26]. Guo *et al.* [20] reported that celastrol affects PC growth by regulating the human ether-a-go-go-related gene channel. However, Song *et al.* [22] determined that celastrol downregulated interleukin-6 gene expression through the nuclear factor kappa-light-chain-enhancer of activated

Journal of
BIOLOGICAL REGULATORS
and Homeostatic Agents

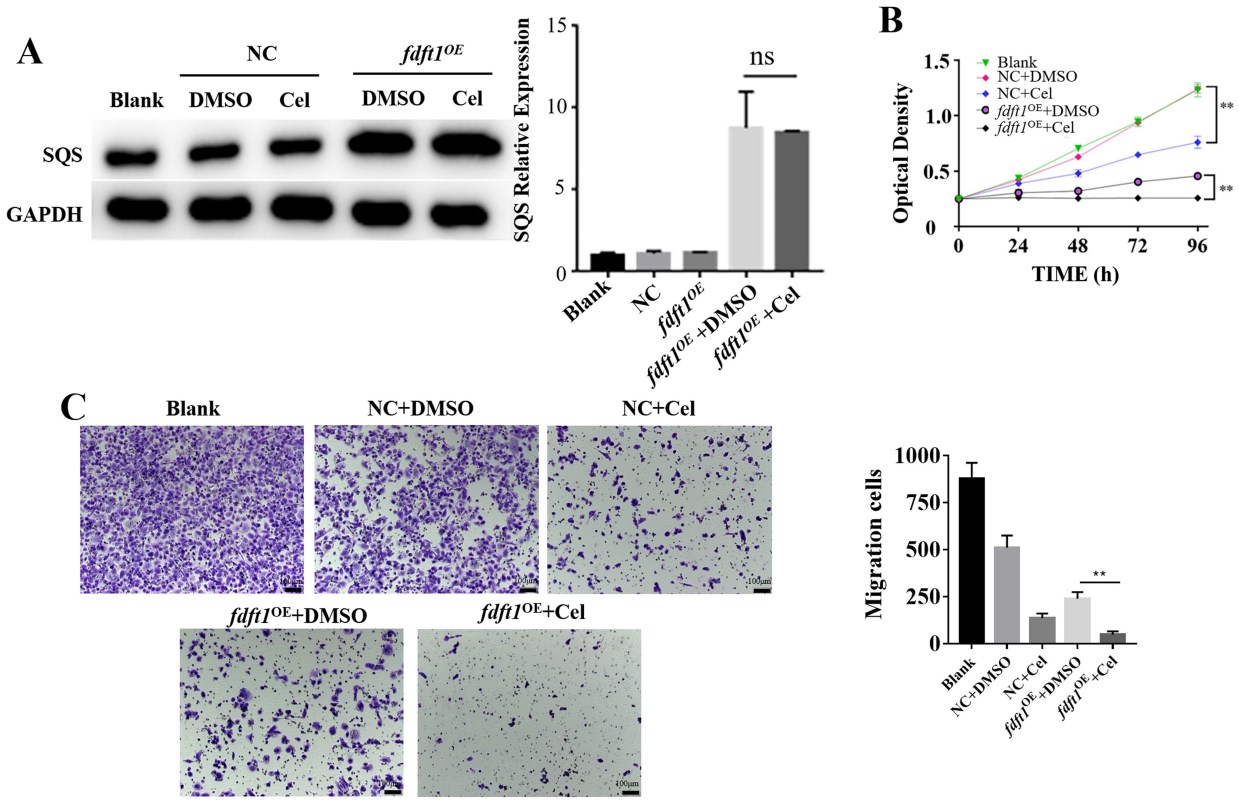

Fig. 6. Effect of overexpression of *fdft1* + celastrol on proliferation and migration of PC cells. (A) PC-3 cells with overexpressed *fdft1* were treated with 2 μM of celastrol, and the changes in SQS levels were observed using Western blot. (B) PC-3 cells with overexpressed *fdft1* were treated with 2 μM of celastrol, and cell proliferation was observed using CCK-8 assay. Transwell experiment: Original magnification ×100. $^{**}p < 0.01$. (C) PC-3 cells with overexpressed *fdft1* were treated with 2 μM of celastrol, and cell migration was observed through a transwell assay. DMSO: control group. Cel: Drug-treated group. Error bars: mean ± SD using two-tailed Student's *t* test analysis, $^{**}p < 0.01$, ns, no significant.

b cell pathway, thereby inhibiting the proliferation of PC-3 cells. Tan Q *et al*. [27] reported that celastrol inhibited PC cells by inducing apoptotic mechanisms. Significantly, the present study found that celastrol reduces the levels of SQS proteins in human cancer cells, which is consistent with recent literature reporting that celastrol reduces the expression of SQS in *Aspergillus* (*A*). *flavus* [22]. Celastrol can inhibit both malignant behaviour and SQS expression, suggesting that the inhibitory effect of celastrol on the malignant behaviours of PC cells may be related to the inhibition of SQS.

To further verify whether the anti-PC effect of celastrol is related to the reduction in SQS, the effect of altering SQS levels on cell malignant behaviour and the anti-cancer effect of celastrol were observed in the present study. A study reported that the downregulation of SQS can inhibit the proliferation of PC cells, but no effect was found on the migration behaviour of these cells [13]. Many studies have determined that SQS is involved in developing different tumours, but the role played by SQS is different in different tumours [29–34]. Jiang *et al*. [30] reported that SQS can promote the progression of colon adenocarcinoma, and Yang *et al*. [31] revealed that SQS can promote the invasion ability of lung cancer cells through the osteopontin/extracellular signal-regulated kinase pathway. However, several studies have demonstrated that SQS can inhibit tumour progression and be a marker for effective patient prognosis [32–34]. We determined that the downregulation of SQS can inhibit the migration of PC cells. Notably, with the overexpression of the *fdft1* gene and upregulation of SQS, the proliferation and migration of PC-3 cells have also decreased. Under overexpression, SQS seems to play a tumour-suppressive role in PC-3 cells. That might be because the overexpression of *fdft1* results in high levels of cholesterol, which not only weakens cell deformation ability but also affects transmission signal molecules, reducing the cell proliferation and migration ability [35]. Moreover, the inhibitory effect of celastrol on SQS proteins was also not evident after *fdft1* overexpression. We suggest this is also associated with lipid metabolism disturbances within cells resulting from *fdft1* overexpression. However, this result needs further confirmation. Nevertheless, the results of the present study suggest that SQS may have a dual effect on the malignant phenotype of PC cells.

In cells with a downregulated or overexpressed *fdft1* gene treated with celastrol, no significant difference was identified in the expression of SQS proteins in the gene-manipulated groups compared with the control groups, but the proliferation and migration of cancer cells were reduced by the addition of celastrol (although the reduction rates were not as severe as in the cells without gene manipulation). Therefore, it can be suggested that the inhibitory effect of celastrol on the malignant phenotype of PC cells is partly dependent on SQS, indicating that the anti-cancer effect of celastrol has other mechanisms independent of SQS [20–22,25], which is consistent with the premise that celastrol is a multi-target anti-cancer drug.

The present study suggests that SQS in PC can be used as a potential therapeutic target and that celastrol could be used as a new SQS inhibitor. However, the study is limited in that only two cell lines and a single dose of celastrol were tested. Further research should therefore be conducted on cell type, animal models, drug concentration and related mechanisms.

Conclusion

This study revealed that celastrol inhibits the proliferation and migration ability of PC cells by decreasing the expression of SQS; the inhibitory effect of celastrol on PC cells partially depends on SQS. Moreover, the knockdown of SQS in PC cells inhibits the proliferation and migration ability. However, the overexpression of SQS in PC-3 cells also inhibits these cells' proliferation and migration ability. The results indicate that SQS may have a dual effect that depends on its expression level. Celastrol could therefore be used as a new inhibitor of SQS to treat PC.

Availability of Data and Materials

All experimental data included in this study can be obtained by contacting the corresponding author if needed.

Author Contributions

Conception and design of the work: LY, YW, and XZ; Data collection: LY, YW, XZ, BP, DZ, YL, FX, SJ, JL, and BC; Supervision: LY, YW and XZ; Analysis and interpretation of the data: all authors; Statistical analysis: LY, YW, XZ, BP, DZ and YL; Drafting the manuscript: LY, YW, XZ, BP, DZ and YL; Critical revision of the manuscript: all authors; Approval of the final manuscript: all authors. All authors have participated sufficiently in the work and agreed to be accountable for all aspects of the work.

Ethics Approval and Consent to Participate

Not applicable.

Acknowledgment

Not applicable.

Funding

Shanghai Pudong New District Youth Talent Project in Medicine (PWRq2020-61). Outstanding Leaders Training Program of Shanghai Pudong New Aera Health Commission (PWRd2018-12).

Conflict of Interest

The authors declare no conflict of interest.

References

[1] Bray F, Ferlay J, Soerjomataram I, Siegel RL, Torre LA, Jemal A. Global cancer statistics 2018: GLOBOCAN estimates of incidence and mortality worldwide for 36 cancers in 185 countries. CA: a Cancer Journal for Clinicians. 2018; 68: 394–424.

[2] Luo GC, Chen L, Fang J, Yan ZJ. Hsa_circ_0030586 promotes epithelial-mesenchymal transition in prostate cancer via PI3K-AKT signaling. Bioengineered. 2021; 12: 11089–11107.

[3] Zhao Y, Tang X, Zhao Y, Yu Y, Liu S. Diagnostic significance of microRNA-1255b-5p in prostate cancer patients and its effect on cancer cell function. Bioengineered. 2021; 12: 11451–11460.

[4] Wang X, Sun B, Wei L, Jian X, Shan K, He Q, *et al*. Cholesterol and saturated fatty acids synergistically promote the malignant progression of prostate cancer. Neoplasia (New York, N.Y.). 2022; 24: 86–97.

[5] Raftopulos NL, Washaya TC, Niederprüm A, Egert A, Hakeem-Sanni MF, Varney B, *et al*. Prostate cancer cell proliferation is influenced by LDL-cholesterol availability and cholesteryl ester turnover. Cancer & Metabolism. 2022; 10: 1.

[6] Kaysudu I, Gungul TB, Atici S, Yilmaz S, Bayram E, Guven G, *et al*. Cholesterol biogenesis is a PTEN-dependent actionable node for the treatment of endocrine therapy-refractory cancers. Cancer Science. 2023; 114: 4365–4375.

[7] Sun L, Ding H, Jia Y, Shi M, Guo D, Yang P, *et al*. Associations of genetically proxied inhibition of HMG-CoA reductase, NPC1L1, and PCSK9 with breast cancer and prostate cancer. Breast Cancer Research: BCR. 2022; 24: 12.

[8] Yousefnezhad M, Davaran S, Babazadeh M, Akbarzadeh A, Pazoki-Toroudi H. PCL-based nanoparticles for doxorubicin-ezetimibe co-delivery: A combination therapy for prostate cancer using a drug repurposing strategy. BioImpacts: BI. 2023; 13: 241–253.

[9] Pandey M, Cuddihy G, Gordon JA, Cox ME, Wasan KM. Inhibition of Scavenger Receptor Class B Type 1 (SR-B1) Expression and Activity as a Potential Novel Target to Disrupt Cholesterol Availability in Castration-Resistant Prostate Cancer. Pharmaceutics. 2021; 13: 1509.

[10] Wang Y, You S, Su S, Yeon A, Lo EM, Kim S, *et al*. Cholesterol-Lowering Intervention Decreases mTOR Complex 2 Signaling and Enhances Antitumor Immunity. Clinical Cancer Research: an Official Journal of the American Association for Cancer Research. 2022; 28: 414–424.

[11] Chen Y, Chen X, Luo G, Zhang X, Lu F, Qiao L, *et al*. Discovery of Potential Inhibitors of Squalene Synthase from Traditional Chinese Medicine Based on Virtual Screening and In Vitro Evaluation of Lipid-Lowering Effect. Molecules (Basel, Switzerland). 2018; 23: 1040.

[12] Dong X, Zhu Y, Wang S, Luo Y, Lu S, Nan F, *et al*. Bava-

chinin inhibits cholesterol synthesis enzyme FDFT1 expression via AKT/mTOR/SREBP-2 pathway. International Immunopharmacology. 2020; 88: 106865.

[13] Fukuma Y, Matsui H, Koike H, Sekine Y, Shechter I, Ohtake N, *et al*. Role of squalene synthase in prostate cancer risk and the biological aggressiveness of human prostate cancer. Prostate Cancer and Prostatic Diseases. 2012; 15: 339–345.

[14] Brusselmans K, Timmermans L, Van de Sande T, Van Veldhoven PP, Guan G, Shechter I, *et al*. Squalene synthase, a determinant of Raft-associated cholesterol and modulator of cancer cell proliferation. The Journal of Biological Chemistry. 2007; 282: 18777–18785.

[15] Werkman IL, Kövilein J, de Jonge JC, Baron W. Impairing committed cholesterol biosynthesis in white matter astrocytes, but not grey matter astrocytes, enhances *in vitro* myelination. Journal of Neurochemistry. 2021; 156: 624–641.

[16] Wang C, Dai S, Zhao X, Zhang Y, Gong L, Fu K, *et al*. Celastrol as an emerging anticancer agent: Current status, challenges and therapeutic strategies. Biomedicine & Pharmacotherapy. 2023; 163: 114882.

[17] Kashyap D, Sharma A, Tuli HS, Sak K, Mukherjee T, Bishayee A. Molecular targets of celastrol in cancer: Recent trends and advancements. Critical Reviews in Oncology/hematology. 2018; 128: 70–81.

[18] Shi J, Li J, Xu Z, Chen L, Luo R, Zhang C, *et al*. Celastrol: A Review of Useful Strategies Overcoming its Limitation in Anticancer Application. Frontiers in Pharmacology. 2020; 11: 558741.

[19] Ji N, Li J, Wei Z, Kong F, Jin H, Chen X, *et al*. Effect of celastrol on growth inhibition of prostate cancer cells through the regulation of hERG channel *in vitro*. BioMed Research International. 2015; 2015: 308475.

[20] Guo J, Huang X, Wang H, Yang H. Celastrol Induces Autophagy by Targeting AR/miR-101 in Prostate Cancer Cells. PloS One. 2015; 10: e0140745.

[21] Chiang KC, Tsui KH, Chung LC, Yeh CN, Chen WT, Chang PL, *et al*. Celastrol blocks interleukin-6 gene expression via downregulation of NF-κB in prostate carcinoma cells. PloS One. 2014; 9: e93151.

[22] Song J, Shang N, Baig N, Yao J, Shin C, Kim BK, *et al*. Aspergillus flavus squalene synthase as an antifungal target: Expression, activity, and inhibition. Biochemical and Biophysical Research Communications. 2019; 512: 517–523.

[23] Picón DF, Skouta R. Unveiling the Therapeutic Potential of Squalene Synthase: Deciphering Its Biochemical Mechanism, Disease Implications, and Intriguing Ties to Ferroptosis. Cancers. 2023; 15: 3731.

[24] Zhang J, Liu D, Deng G, Wang Q, Li L, Zhang J, *et al*. lncRNA prostate cancer-associated transcript 18 upregulates activating transcription factor 7 to prevent metastasis of triple-negative breast cancer via sponging miR-103a-3p. Bioengineered. 2021; 12: 12070–12086.

[25] Cao L, Zhang X, Cao F, Wang Y, Shen Y, Yang C, *et al*. Inhibiting inducible miR-223 further reduces viable cells in human cancer cell lines MCF-7 and PC3 treated by celastrol. BMC Cancer. 2015; 15: 873.

[26] Guo J, Mei Y, Li K, Huang X, Yang H. Downregulation of miR-17-92a cluster promotes autophagy induction in response to celastrol treatment in prostate cancer cells. Biochemical and Biophysical Research Communications. 2016; 478: 804–810.

[27] Tan Q, Liu Z, Gao X, Wang Y, Qiu X, Chen J, *et al*. Celastrol recruits UBE3A to recognize and degrade the DNA binding domain of steroid receptors. Oncogene. 2022; 41: 4754–4767.

[28] Sanna V, Chamcheu JC, Pala N, Mukhtar H, Sechi M, Siddiqui IA. Nanoencapsulation of natural triterpenoid celastrol for prostate cancer treatment. International Journal of Nanomedicine. 2015; 10: 6835–6846.

[29] Karakitsou E, Foguet C, Contreras Mostazo MG, Kurrle N, Schnütgen F, Michaelis M, *et al*. Genome-scale integration of transcriptome and metabolome unveils squalene synthase and dihydrofolate reductase as targets against AML cells resistant to chemotherapy. Computational and Structural Biotechnology Journal. 2021; 19: 4059–4066.

[30] Jiang H, Tang E, Chen Y, Liu H, Zhao Y, Lin M, *et al*. Squalene synthase predicts poor prognosis in stage I-III colon adenocarcinoma and synergizes squalene epoxidase to promote tumor progression. Cancer Science. 2022; 113: 971–985.

[31] Yang YF, Chang YC, Jan YH, Yang CJ, Huang MS, Hsiao M. Squalene synthase promotes the invasion of lung cancer cells via the osteopontin/ERK pathway. Oncogenesis. 2020; 9: 78.

[32] Zhao R, Cao B, Li H, Li T, Xu X, Cui H, *et al*. Glucose starvation suppresses gastric cancer through targeting miR-216a-5p/Farnesyl-Diphosphate Farnesyltransferase 1 axis. Cancer Cell International. 2021; 21: 704.

[33] Nakae A, Kodama M, Okamoto T, Tokunaga M, Shimura H, Hashimoto K, *et al*. Ubiquitin specific peptidase 32 acts as an oncogene in epithelial ovarian cancer by deubiquitylating farnesyl-diphosphate farnesyltransferase 1. Biochemical and Biophysical Research Communications. 2021; 552: 120–127.

[34] Huang R, Zhang C, Wang X, Zou X, Xiang Z, Wang Z, *et al*. Identification of FDFT1 as a potential biomarker associated with ferroptosis in ccRCC. Cancer Medicine. 2022; 11: 3993–4004.

[35] Ha NT, Lee CH. Roles of Farnesyl-Diphosphate Farnesyltransferase 1 in Tumour and Tumour Microenvironments. Cells. 2020; 9: 2352.